Locally excited coupled map lattice: Phase transition from a local to a global response

Gang Hu,[1,2] Fagen Xie,[3] Zhilin Qu,[2] and Fang Zhang[2]
[1]*China Center of Advanced Science and Technology, (World Laboratory), Beijing, P.O. Box 8730, China*
[2]*Department of Physics, Beijing Normal University, Beijing 100875, China*
[3]*Institute of Theoretical Physics, Academia Sinica, Beijing 100080, China*
(Received 1 January 1996)

A coupled map lattice system is perturbed by a local injection. The system response to the external excitation is investigated. We find a phase transition from local response to a global response. As global response functions the motions of the sites far from the forced site show critical on-off intermittency. The implication of the global response to the physical transportation behavior is addressed. [S1063-651X(96)11108-9]

PACS number(s): 05.45.+b

I. INTRODUCTION

In recent years, much attention in the field of nonlinear science has been shifted to spatiotemporal systems. The extremely rich behavior of bifurcations, patterns, spatiotemporal chaos, and fully developed turbulence, and the control of these objects have become rather active topics. As the simplest model of spatiotemporal systems, the coupled-map-lattice system (CML) has been extensively investigated over the recent decade [1–9]. On one hand these CML systems can be regarded as time-space discretizations of continuous extended physical systems. Therefore, from the investigations of these simplest models we can understand the rich behaviors of much more complicated realistic systems. On the other hand, some practical systems (such as generation iterations of biology population distribution) may be represented directly by space-time maps, then the CML models are of great importance in their own right. However, one point of theoretical importance and practical significance has, to our knowledge, escaped the scope of numerous investigations: how does the CML system respond to an external excitation or, in other words, how does a local perturbation alter the entire nonlinear spatiotemporal system through couplings. The present paper is devoted to this subject.

Specifically, we use the following model as our working example:

$$x_{n+1}(i)=(1-\epsilon)f(x_n(i))+\left(\frac{\epsilon}{2}+C\right)f(x_n(i-1)) +\left(\frac{\epsilon}{2}-C\right)f(x_n(i+1)), \tag{1}$$

where the mapping function $f(x)$ is defined as the logistic map $f(x)=ax(1-x)$. We use a periodic boundary condition $x_n(i)=x_n(i+L)$, with L being the lattice length. The quantities ϵ and C have clear physical meanings; the former represents the diffusion strength while the latter the asymmetric force, or say, a gradient bias. Changing a, ϵ, and C, the system exhibits very rich patterns, which have been demonstrated in numerous papers. In Sec. II we focus our attention on a symmetric CML, i.e., on the parameter region $a=4$, $C=0$, $0.1394<\epsilon<0.1938$, where the system has a single time-period-2 and space-period-2 (T2S2) attractor with even L. A phase transition from a local response to a global one, associated with a spatiotemporal intermittency, is observed when we inject and increase the local excitation. In Sec. III we consider the asymmetric CML with nonzero C. Similar behavior is also found. An interesting excitation transport forced by gradient bias is clearly seen. In Sec. IV a local excitation is injected into a spatiotemporal chaotic state; we again find the transition from local response to global excitation. Some discussion about the mechanism underlying the intermittency effect will be given in Sec. V.

II. SPATIOTEMPORAL INTERMITTENCY BASED ON A T2S2 STATE OF SYMMETRIC CML

The stable T2S2 state at $L=300$, $\epsilon=0.15$, and $C=0$ is shown in Fig. 1(a), which can be asymptotically (rather quickly) approached from different random initial conditions. Now we start to investigate the response of the system to an external perturbation. To do that we modify Eqs. (1) to

$$\overline{x_n}(i)=\begin{cases} x_n(i) & \text{if } x_n(i)+\sigma\delta_{i,\frac{L}{2}+1}\geqslant 1, \\ x_n(i)+\sigma\delta_{i,L/2+1} & \text{otherwise,}\end{cases}$$

$$x_{n+1}(i)=(1-\epsilon)f(\overline{x_n}(i))+\left(\frac{\epsilon}{2}+C\right)f(\overline{x_n}(i-1)) +\left(\frac{\epsilon}{2}-C\right)f(\overline{x_n}(i+1)). \tag{2}$$

In Eqs. (2) the constant control parameter σ represents the strength of the external perturbation injected to the $(L/2)+1$st site. In Fig. 1 we show the system responses for different σ. Several features are interesting as well as surprising.

In Fig. 1(b) we plot the asymptotic behavior of the forced site $x_n(151)$ against σ. A clear period-doubling cascade leading to chaos is found. In the chaotic region we find obvious period windows. All other unforced sites also follow the characteristic bifurcation behavior of the forced site. In Fig. 1(c) $x_n(145)$ has similar bifurcation features like Fig. 1(b), which can be clearly seen by a proper amplification of the plots. The most interesting point is the existence of period windows [for a more clear view, see Fig. 1(d)] in the large (i.e., large L) CML system. To date, for large CML systems, to our knowledge, systematic appearances of period

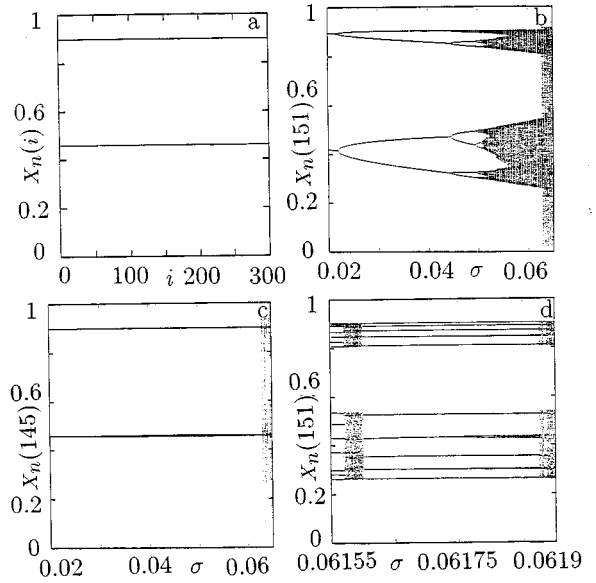

FIG. 1. (a) The asymptotic state of the CML, Eqs. (1) [or Eqs. (2) at $\sigma=0$], at $a=4$, $\epsilon=0.15, C=0$, and $L=300$. The same parameters are taken in Figs. 1–3. The initial condition is that each site takes a random number in the interval [0, 1]. The figure is plotted by 300 iterations after the transient process. A single stable T2S2 attractor is identified. (b) $x_n(151)$ vs σ after the transient process is excluded. At $\sigma=\sigma_c=0.0622$, a crisis of chaotic region expansion occurs. (c) $x_n(145)$ vs σ after the transient process is excluded. As $\sigma<\sigma_c$, the deviation from the T2S2 state of (a) is small. However, after $\sigma>\sigma_c$, a burst of deviation is observed. (d) A blowup of a periodic window region in (b). The same window can be seen in chaotic regions for each site in the same parameter regime.

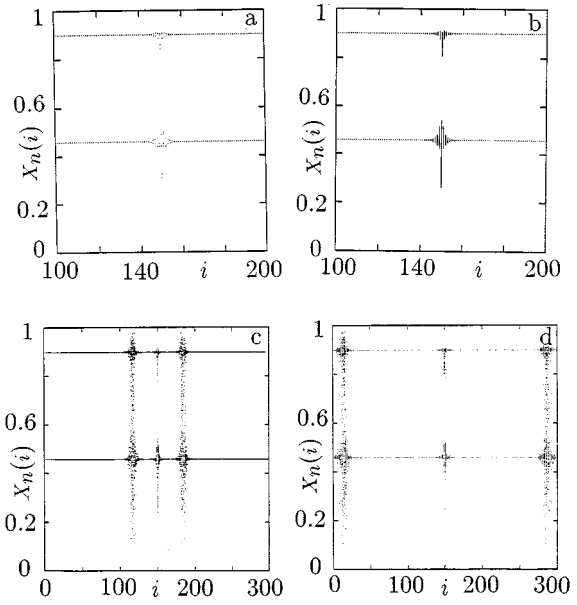

FIG. 2. (a) $x_n(i)$ data plotted for each site in 1500 iterations at $\sigma=0.048$ after the transient process. The envelope of the deviations from T2S2 is frozen. (b) The same as (a) with σ replaced by $\sigma=0.062$. The deviation envelope is also frozen and the response of the system to the excitation is local. (c) The same as (a) with $\sigma=0.063$. The plotted iterations are from $n=42\,000$ to $n=42\,300$. Clusters of bursts from the basic state of (b) can be observed. (d) The same as (c) with plotted iterations being from $n=1.42\times10^5$ to $n=1.423\times10^5$. The clusters of excitons move too far away from the forced site.

windows in the chaotic region have not been found (apart from some parameter regimes of extremely weak coupling, $\epsilon=0$ or $\epsilon\ll1$). By perturbing a single site we find period windows in a rather regular way. These windows are dynamically stable against arbitrary random initial preparations and structurally stable against small perturbation of control parameters.

Comparing Figs. 1(b) and 1(c), it is clear that the constant forcing at the central site drives the forced site as well as unforced ones away from the unperturbed T2S2 state of Fig. 1(a). However, the deviations of the motions of different sites from the unperturbed state are different. As $\sigma<0.0622$, the farther a site locates from the forced site, the smaller the deviation. This feature is clearly shown in Figs. 2(a) and (b). Actually, for the $(L/2+1\pm m)$th site the deviation is no longer visible as $m>10$, no matter whether the motion is periodic [Fig. 2(a)] or chaotic [Fig. 2(b)]. The influence of the external excitation is local. It can affect only the motions of the sites in the neighborhood of the forced site. The deviations caused by the forcing damps exponentially as the site distance m increases. An empirical formula

$$|x(L/2+1\pm m)-\hat{x}|\leqslant|\mathbf{A}(\sigma)|e^{-\beta m}, \tag{3}$$

well fit the actual deviation from the lower line of Fig. 1(a) for both periodic and chaotic states. In Eq. (3), $\hat{x}=(x_1,x_2)$ is the T2S2 state. The envelopes of the deviation shown in Fig. 2(a) or 2(b) are time independent. After short transient iterations, the envelopes are asymptotically approached and frozen forever. The amplitude of $\mathbf{A}(\sigma)=(A_1,A_2)$ depends on the forcing strength. The decay exponent β is independent of the values of σ and L (if L is large enough and σ is not too large, of course), but depends on ϵ, a, and the way in which the sites couple to each other (e.g., nearest-neighbor coupling, or next-nearest-neighbor coupling, or etc). At the parameters of Fig. 1 we find $\beta\approx0.52$. Actually, the exponent β can be calculated exactly. The main points for computations are the following. First, as $|i-L/2-1|$ is large, linearization of the derivations from the period-2 state can be valid. In the linear case margin certainly maps to margin. Therefore, the margin is a stationary period 4 state of the system. Inserting Eq. (3) to the linearized Eq. (1) we immediately obtain

$$\begin{aligned} &a(1-\epsilon)(1-2x_1)A_1-[a\epsilon(1-2x_2)\sinh\beta+1]A_2=0,\\ &[a\epsilon(1-2x_1)\sinh\beta+1]A_1+a(1-\epsilon)(1-2x_2)A_2=0, \end{aligned} \tag{4}$$

leading to the condition

$$\begin{vmatrix} a(1-\epsilon)(1-2x_1) & -[a\epsilon(1-2x_2)\sinh\beta+1] \\ [a\epsilon(1-2x_1)\sinh\beta+1] & a(1-\epsilon)(1-2x_2) \end{vmatrix}=0, \tag{5}$$

from which β can be given analytically. At $a=4$, $\epsilon=0.15$, we have $x_1=0.458\,414$ and $x_2=0.898\,729$, and then get $\beta\approx0.52$, which is confirmed by numerical simulations.

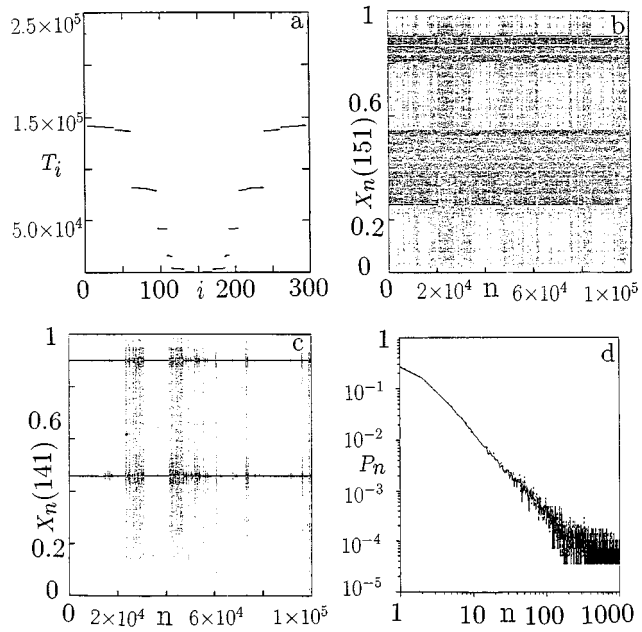

FIG. 3. (a) T_i plotted against i. T_i is the iteration number for the ith site to be excited for the first time. [A site is regarded to be excited as $|x_n(i)-\hat{x}|>0.03$, where $\hat{x}$ is the T2S2 state of the unperturbed system.] The T_i behavior is very similar to that of random walks. (b) $x_n(151)$ plotted vs n; the motion seems to be of on-off intermittency. (c) The same as (b) for $x_n(141)$, a motion of typical on-off intermittency. (d) The distributions of laminar phases for 141st and 131st sites. A perfect $-\frac{3}{2}$ power-law decay is identified. The solid and dashed lines represent those of 141st and 131st sites, respectively.

The final and the most important feature is that there exists a characteristic change, or say, a phase transition in the system response to the excitation, which happens at $\sigma_c=0.0622$. The system behaviors for $\sigma<\sigma_c$ and $\sigma>\sigma_c$ are totally different [see Figs. 2(b) and 2(c)]. In the former case, the sites far from the forced site stay in the vicinity of the unperturbed T2S2 state, and the system response to the excitation has a local nature, obeying the restriction Eq. (3). However, in the latter case, even the sites far away from the forced one may wander in the entire variable space. The law of local response of Eq. (3) is completely broken. The system response to a local injection is global. In order to confirm the transition from a local to a global response, we present Figs. 2(c) and 2(d), where we plot the system state for two different time periods in the same manner as Figs. 2(a) and 2(b). Two major differences between these two types of figures, which have fundamental significance in practice, can be seen. First, in Figs. 2(c) and 2(d), the envelope of the deviations from the T2S2 state is no longer frozen. It seems that the excited sites (called excitons) form a centralized cluster; this cluster keeps moving and wanders in space like a Brownian particle. In Fig. 3(a) we plot the time T against i, where T_i is the time for the ith site to get excited [i.e., $|x_n(i)-\hat{x}|$ becomes larger than 0.03] for the first time. These first passage time plots are very similar to those of the random walk. Second, in Figs. 2(c) and 2(d) the influence of the local excitation is global. The cluster of excitons may walk, in a random manner, to full lattice length. We have tried $L=500$ and $L=1000$. In all cases, we find all sites can be excited, though it takes a long time for the excitons to propagate to the sites very far from the central site. On the contrary, in Figs. 2(a) and 2(b) the influence is purely local, as we described previously. The only difference between the control parameters of Figs. 2(d) and 2(b) is that $\sigma=0.062$ for the latter and 0.063 for the former. A slight change in the control parameter induces an essential change of the system behavior; this convinces us of the existence of a phase transition from a local response to a global response. We would like to emphasize that the property of global response is of crucial importance for realistic network systems. If global response is identified, on one hand, one may detect an external signal from a large distance; on the other hand, one may effectively influence and control large extended systems by a local injection. In both cases the applications of this global response are unlimited.

To further investigate the characteristic features of the motion of the system for $\sigma>\sigma_c$, we record the time evolutions of the 151st and 141st sites in Figs. 3(b) and 3(c). The motion of (c) is of typical on-off intermittency [10–14]; i.e., it stays at the ''off'' state for a very long time, and suddenly departs quickly from, and then returns quickly to, the ''off'' state. The ''off'' state is defined by Eq. (3). In Fig. 3(d) we plot the scaling property of the probability P_n for the 141st and 131st sites, where P_n represents the probability of the laminar phase of length n, namely, $P_n=M_n/N$, with N being the total number of the segments of the laminar phase, and M_n the number of that of length n. The threshold for the laminar phase is defined as

$$|x(i)-\overline{x(i)}|<\tau=10^{-3}, \tag{6}$$

where $\overline{x(i)}$ is given by Eq. (3), i.e., the ''off'' state. The definition of the laminar phase for the other cases is also given by Eq. (6). But the ''off'' state $\overline{x(i)}$ is different from the others. The scaling curves show perfect $-3/2$ power-law decay of the connected time length of the off state; that further confirms the critical on-off intermittency. We have also tried $i=121$ and $i=101$, and got the same scaling curve. There are several points worth making for the on-off intermittency in our model. First, to drive the system to an on-off intermittency state we vary a constant force σ rather than a noise force; thus the control parameter is *static* rather than *dynamic*. Second, when the on-off intermittency occurs the off state of the system is *spatiotemporal chaos* rather than a *static* or *periodic* state. This basic chaotic state offers a dynamic origin for the on-off intermittency. Third, in our extended system, the on-off criticality can be self-organized. Precisely, as $\sigma>\sigma_c$ (not equal to σ_c), the time evolutions of the forced site and some near sites do not obey the $-\frac{3}{2}$ power law. An exponential decay tail increases as $\sigma-\sigma_c$ increases. As the distance of sites from the forced site increases, the scaling behavior of these sites becomes closer to the $-\frac{3}{2}$ power law even at large $\sigma-\sigma_c$. As the distance $|i-L/2-1|$ is sufficiently large, all sites show perfect $-\frac{3}{2}$ power-law behavior shown in Fig. 3(d). Therefore, the on-off intermittency criticality can be organized by the system itself through the mutual coupling. The final important point is that local response changes to global response exactly at the mo-

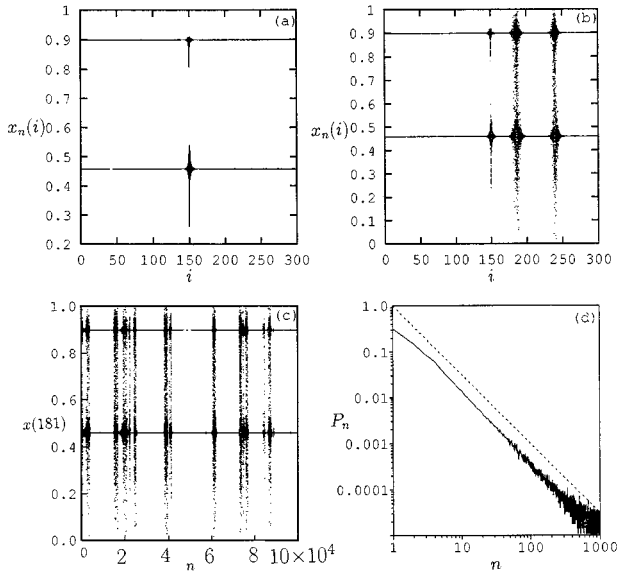

FIG. 4. (a) The same as Fig. 2(b) with C replaced by $C=0.0075$. A small bias can only slightly change the shape of the envelope of the chaotic region. The envelope is still frozen. (b) The same as Fig. 2(c) with $C=0.0075$, the plotted iterations are from $n=21\,900$ to $n=22\,100$. The clusters of excitons are pushed to the right, and move far away from the forced site in a much shorter time [in comparison with Figs. 2(c) and 2(d)]. Thus the transportation property is entirely changed by the small bias in the global response case. (c) $x_n(181)$ plotted vs n. The nature of on-off intermittency is preserved after bias. (d) The distribution of laminar phase for (c). Perfect $-\frac{3}{2}$ power-law decay is still prevailing. The dashed line is the perfect $-\frac{3}{2}$ power-law decay. The dashed lines in the following figures have the same mean.

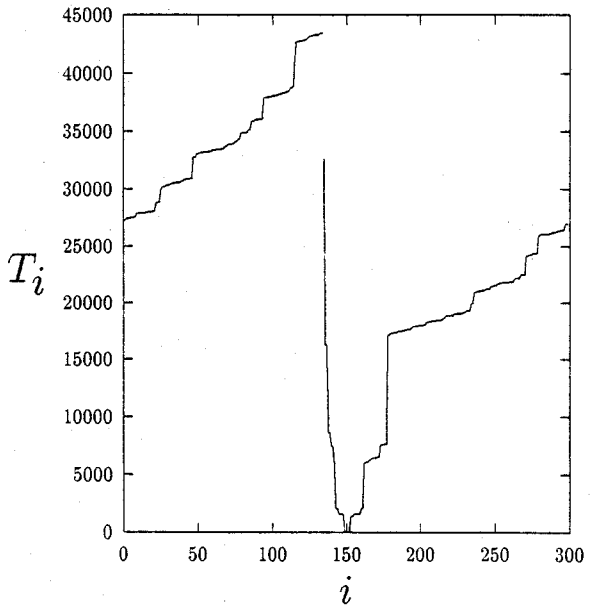

FIG. 5. The same as Fig. 3(a) except $C=0.0075$. Clusters of bursts make biased random walks.

ment when the normal chaotic state [shown in Fig. 2(b)] is replaced by the on-off intermittency state. Therefore, there is an intimate relation between these two interesting transitions, the phase transition from a local response to a global one and the phase transition to spatiotemporal intermittency. Nevertheless, the mechanism underlying this link is unknown and should be further investigated.

III. SPATIOTEMPORAL INTERMITTENCY BASED ON T2S2 STATE IN ASYMMETRIC CML

At $\sigma>\sigma_c$, and $C=0$, excitons may move too far away from the forced site by random walks. However, the time for excitons to move to $i=1$ (or $i=L$) is very long as L is large. A small bias [nonzero C in Eqs. (2)] provides a constant force to these excitons and greatly reduces the propagation time. In Fig. 4(a) we do the same computation as in Fig. 2(b) except we replace $C=0$ with $C=0.0075$. The bias does not much change the system dynamics: the system is still chaotic and the response of the system to the local excitation is still local. The only difference between Figs. 4(a) and 2(b) is that the symmetry (between $i-L/2-1$ and $L/2+1-i$) of the envelope existing in Fig. 2(b) is broken in Fig. 4(a). In Fig. 4(b) we do the same thing as in Figs. 2(c), except we replace $C=0$ by $C=0.0075$. With this small bias clusters of excitons move to the sites far away from the forced site in time much smaller than that without bias [2.2×10^4 iterations for Fig. 4(b) while 1.4×10^5 iterations for Fig. 2(d)]. It seems that clusters of excitons are pushed by a constant force to the right as they make random walks. From Figs. 4(a) and (4(b) it is clear that the transportation property is not much changed by bias in the local response case, while in the global response case a small bias may totally change the transportation characteristics of the system by yielding a finite mobility of the excited defects. In the case of $C\neq0$ we again find that the motions of the sites are of on-off intermittency [see Fig. 4(c)], and for the sites far away from the forced site the scaling property of the off state distribution is the same as that shown in Fig. 3(d), namely, $-\frac{3}{2}$ power-law decay [see Fig. 4(d)]. Here the ''off'' state is the asymmetric spatiotemoral chaos shown in Fig. 4(a). In Fig. 5 we perform the same computation as in Fig. 3(a). A biased random walk is obvious, and the time for excitons to move a large distance is much shortened in comparison with the random walk in the symmetric CML case.

Changing the bias C may essentially change the dynamics of the system. In Fig. 6 we take a considerably large C ($C=0.04$). From Fig. 6(a) to Fig. 6(d) we gradually increase the local injection σ. At $\sigma=0$, we still have a stable T2S2 state [Fig. 6(a)]. Increasing σ, we first find an interesting phenomenon of state splitting [Fig. 6(b)]: the original T2S2 state bifurcates to a T4S4 state. In Fig. 6(c), by further increasing σ, the T4S4 state is replaced by a chaotic state. Nevertheless, the deviation from the T4S4 state again decays exponentially as the site distance from the forced site increases. In Fig. 6(d) we find a global chaos band merge via spatially global crisis. The patterns and bifurcations shown in Fig. 6 have some features essentially different from those in Figs. 1(a)–1(c). When we further increase σ to $\sigma>\sigma_c\approx0.0665$, we find random bursts from the two chaotic bands, which start from the forced site and propagate to the right very quickly. In Figs. 7(a) and 7(b) we plot the iterations for each site from $n=1500$ to $n=1600$, and from

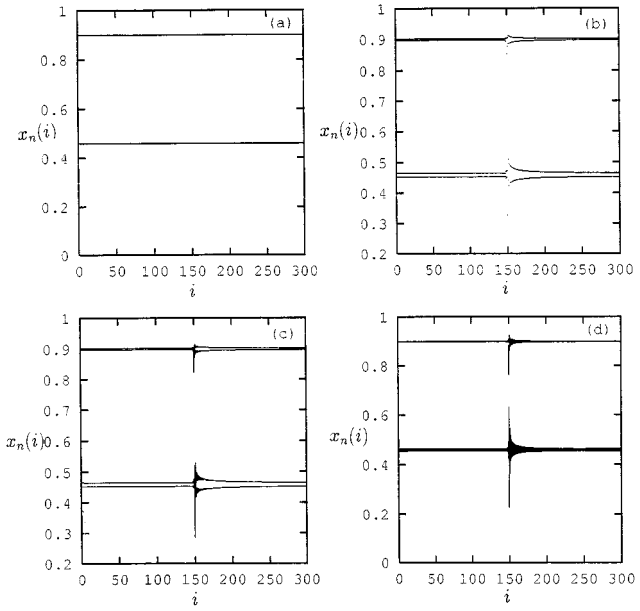

FIG. 6. $a=4$, $\epsilon=0.15$, and $C=0.04$. (a) $\sigma=0$. The figure is plotted in the same way as Fig. 1(a). The same T2S2 state is asymptotically approached from random initial preparations. (b) $\sigma=0.042$. Global state split is observed; that is sharply different from the behavior of Fig. 2(a). (c) $\sigma=0.054$. The system state is chaotic. (d) $\sigma=0.066$. Four chaotic bands fairly merge to two bands.

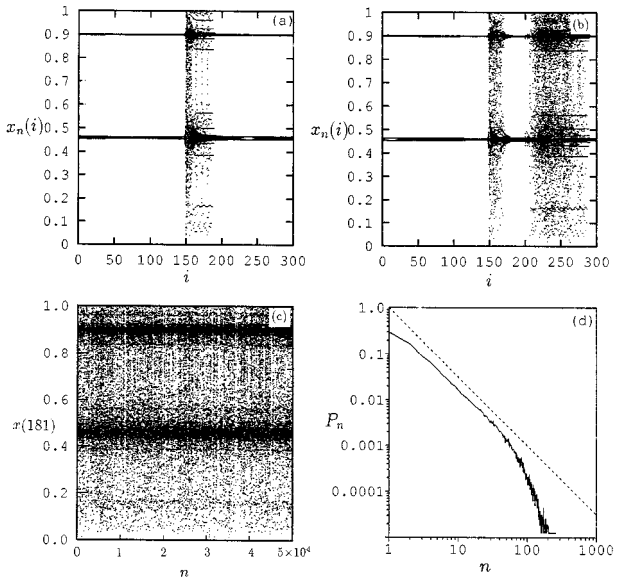

FIG. 7. $\sigma=0.067$. All other parameters are the same as in Fig. 6. (a) All data of iterations from $n=1500$ to 1600 are plotted. Chaotic bursts from the chaotic bands Fig. 6(d) are excited from the forced site. (b) All data of iterations from $n=1700$ to 1900 are plotted. Excitons are quickly created and move to the right. (c) $x_n(181)$ plotted vs n. A trace of on-off intermittency can be still seen, but large laminar phase segments can hardly be observed. (d) The laminar phase distribution of (c). One finds a large $-\frac{3}{2}$ power-law scaling segment followed by an exponential decay tail.

$n=1700$ to $n=1900$, respectively. Some features are worth-discussing. First, the clusters of excitons are well centralized in Figs. 2(c), 2(d), and 4(c) while they become much less centralized in Figs. 7(a) and 7(b). The quick creations and quick propagations of bursts (caused by large C) weaken and destroy the centralized form, and make bursts distributed in a wide space region. Nevertheless, the feature observed in Figs. 2(c), 2(d), and 4(c) that all sites far away from the forced site spend most of time in the vicinity of the chaotic bands of Fig. 6(d) (then the bursts must be quickly excited and quickly annihilated) can be still found in Figs. 7(a) and 7(b). This feature is a characteristic of intermittency. In Fig. 7(c) we plot the time evolution of $x_n(181)$ against n; the intermittency nature can be again clearly seen. In Fig. 7(d) we plot the laminar phase distribution of the time series of Fig. 7(c). The ''off'' state for this case is the asymmetric spatiotemporal chaos in Fig. 6(d). The large linear segment shows $-\frac{3}{2}$ power-law scaling caused by the on-off intermittency of the system dynamics, and the exponential decay in the large n side indicates that the laminar phase can hardly persist for a long time due to the quick propagation of bursts for large C.

IV. EXCITATIONS FROM A BASIC SPATIOTEMPORAL CHAOTIC STATE AND THEIR PROPAGATIONS

In the previous sections we found a phase transition of the system response to a local injection from a local to a global response, associated to a spatiotemporal on-off intermittency, when the system takes a T2S2 periodic wave state without excitation ($\sigma=0$). It is interesting to ask whether the effect is generic; i.e., can we find a similar phenomenon in wider parameter regions? In particular, can we find the same type of response behavior when the system state is spatiotemporal chaos without external injections? In this section, we come back to the symmetric CML. With $C=0$, the dynamical behavior of Eqs. (1) has been extensively investigated. It is well known that the system state is spatiotemporal chaos at $a=4$ and $\epsilon=0.125$. In Fig. 8(a) we take $L=300$, and plot the asymptotic state of the system. Now we inject an external force on the site $i=151$; the responses of different sites are shown in Figs. 8(b)–8(d). From these plots we find some interesting features. By local injection we can effectively suppress spatiotemporal chaos in a certain parameter region ($0.0117\approx\sigma_1<\sigma<\sigma_2\approx0.0264$). It is really surprising that a simple constant injection at a single site can play so effective a role in suppressing chaos in the entire extended system. This point will be further investigated in our future works. At $\sigma_2\approx0.0264$, there is a jump (phase transition) to spatiotemporal on-off intermittency. As $\sigma>\sigma_2$, bursts are excited from the forced cell, and can propagate in the entire spatial medium; that is similar to the behavior of Figs. 2(c) and 2(d).

We take $\sigma=0.0265$ as an example. In Figs. 9(a) and 9(b) we present space-time plots produced in the same way as in Figs. 2(c) and 2(d). We find similar clusters of bursts. These clusters start from the forced cell and wander too far away in the manner of random walk. In Fig. 9(c) we plot the time series of the site $i=131$; the on-off nature of intermittency is clear. The essential difference between Fig. 9(c) and all the previous time series of on-off intermittency is that now the basic ''off'' state (laminar phase) is characterized by spatiotemporal chaos bands with large width. In Fig. 9(d) we

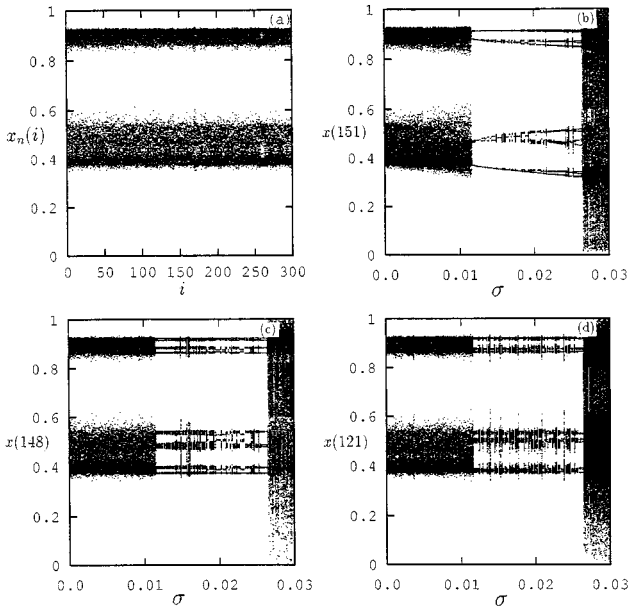

FIG. 8. $a=4$, $C=0$, $\epsilon=0.125$, and $L=300$. (a) $\sigma=0$, the spatiotemporal chaotic state of Eq. (1). The figure is plotted by 100 iterations after the transient process. Two chaotic bands are asymptotically approached. (b) $x_n(151)$ vs σ after the transient process is excluded. In the region $0.0117\approx\sigma_1<\sigma<\sigma_2\approx0.0264$ chaos is effectively suppressed. At $\sigma=\sigma_2$ a crisis of the chaotic region expansion occurs. (c) $x_n(148)$ vs σ after the transient process. Characteristic changes at both σ_1 and σ_2 can be found. (d) $x_n(121)$ vs σ after the transient process. Chaos is still effectively suppressed in the region $\sigma_1<\sigma<\sigma_2$. At σ_2, a burst to large scale chaotic motion occurs.

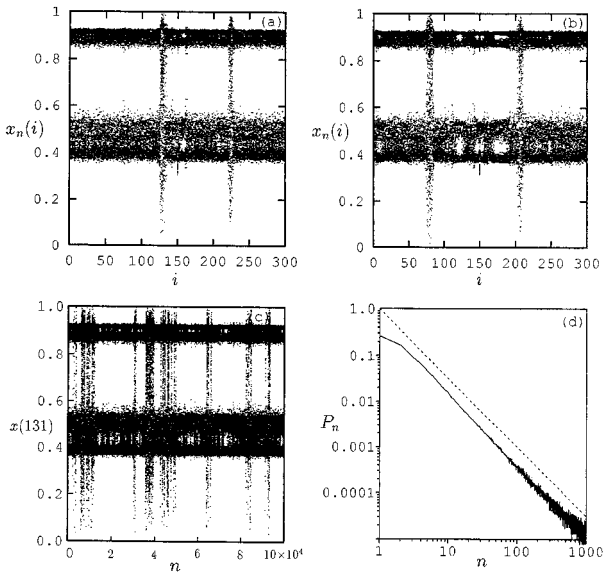

FIG. 9. $\sigma=0.0265$; the other parameters are the same as in Fig. 8. (a) All data of iterations from $n=58\,000$ to $58\,100$ are plotted. Some clusters of bursts excited from the basic chaotic bands of Fig. 8(a) can be observed. (b) The same as (a) except the iterations being from $n=70\,000$ to $70\,100$. Exciton clusters make random walks. (c) $x_n(131)$ plotted vs n. On-off intermittency is obvious. (d) The laminar phase distribution of (c). The spatiotemporal state of Fig. 8(a) is regarded as the laminar phase state.

plot the laminar phase distribution of (c); a perfect $-\frac{3}{2}$ power law scaling is identified. This critical power law can be equally found for all cells with $|i-151|\gg1$. It is worthwhile remarking that the global response of the system to local injection appears before the on-off intermittency in Fig. 8 (even in Fig. 6 in a strict sense). However, the global exciton propagations (random walks in Fig. 9 and biased walks in Fig. 7) are obviously related to on-off intermittency.

V. MECHANISM AND SELF-EXCITED CML SYSTEMS

The features, a phase transition of the system response to a local injection from local response to global response, and on-off intermittency after the phase transition, are rather generic. They are observed for both symmetric and asymmetric CML's, and found in different parameter regions when the system states without the injection can be both regular (periodic) and chaotic. It is emphasized that the generic features are not sensitive to the nature of the injection. For instance, if we replace the constant force σ in Eqs. (2) by a stochastic force, the same phenomena can be observed as well [14].

In the discussions of the previous sections, a feature of self-organized criticality is also worthwhile remarking upon. The laminar phase distributions of the time series of sites near the forced site have clear exponential decay in the large time regime. However, with $|C|\ll1$ for the sites far from the forced cell the laminar phase distributions show, identically, perfect $-\frac{3}{2}$ power-law scaling, i.e., manifest behavior that is expected to occur at a critical point of phase transition to on-off intermittency. This criticality is *self-organized* during the propagation of excitons.

It is important to reveal the mechanisms underlying all of the above significant features. Up until now, we had no clear answers. Nevertheless, a heuristic explanation of self-organized criticality of the on-off intermittency may be the following. The critical $-\frac{3}{2}$ power-law scaling is an intrinsic behavior of the coupled system, irrelevant to the external injection. Injection plays the role only stimulating the sites away from the ''off'' state and maintaining excitation by continuously injecting ''energy.'' The sites near the forced one are strongly influenced by the injection and exhibit a clear exponential tail of laminar phase length distribution, while the dynamics of sites far from the forced site is much less influenced by the injection and keeps the intrinsic feature of the system, exhibiting a pure $-\frac{3}{2}$ power-law decay. Comparing the bursts (from periodic states or laminar chaotic bands) in this paper with the defects in Refs. [5,15,16], we find that the former mechanism is very similar to the latter. In our case defects are continually created from the forced site and propagate too far away. What we have essentially advanced from Ref. [5] is that weak local forcing cannot affect the global behavior of the spatiotemporal system (or, say, small defects excited by the injection cannot propagate in the medium); there is a phase transition to global response characterized by the large distance propagation of defects.

The above explanation of the mechanism of self-organized criticality of on-off intermittency can be convincingly confirmed by the following self-excited CML models. In the previous sections we always took even L, then laminar

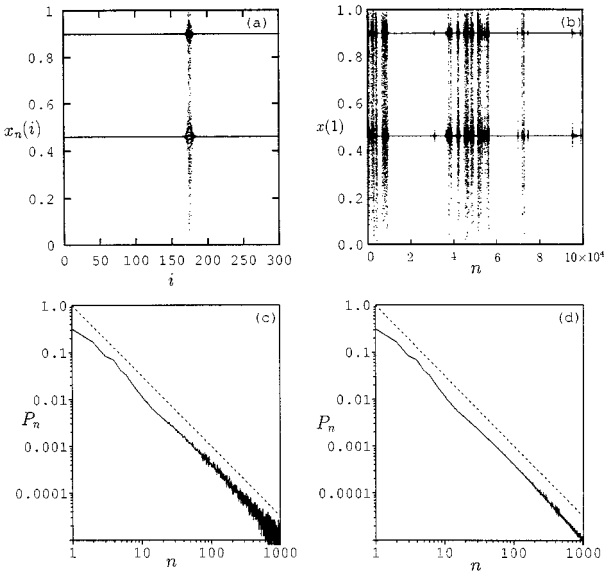

FIG. 10. $\sigma=0$, $L=301$, all other parameter are the same as in Fig. 1. (a) After transient process we plot data of 100 iterations. Centralized clusters of bursts from the basic T2S2 state can be clearly observed. (b) $x_n(1)$ plotted vs n. On-off intermittency from T2S2 state is obvious. (c) Laminar phase distribution of (b). Perfect $-\frac{3}{2}$ power-law scaling is observed. (d) The laminar phase distribution averaged from all the 301 sites. The distribution is essentially the same as Fig. 10(c) with fewer fluctuations.

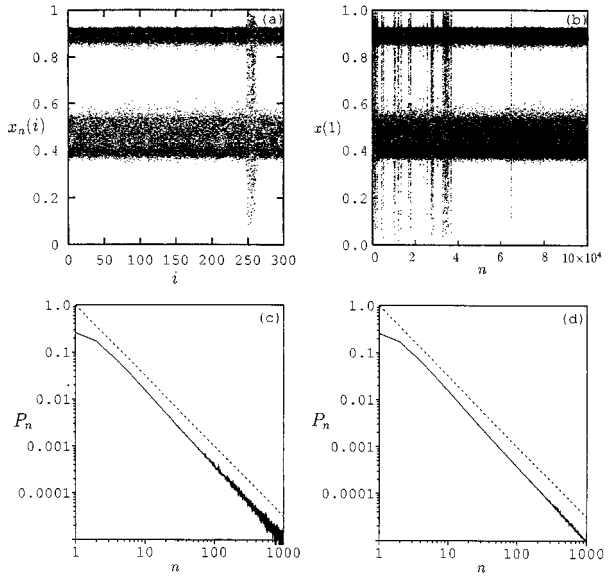

FIG. 11. (a)–(d) are produced in exactly the same way as Figs. 10(a)–10(d), respectively, except that the coupling is changed to $\epsilon=0.125$ at which the laminar phase is a spatiotemporal chaos rather than the T2S2 periodic state. It is surprising that adding one more site to the system of Fig. 8(a) can change the system dynamics so significantly.

phase states are stable, and instability to on-off intermittency is induced by an external local injection. What happens when we take odd L? It is clear that if we take all the same parameters as those in Fig. 1(a), except replacing $L=300$ by 301, the T2S2 state cannot be stable due to mismatch of odd number of sites. With $a=4$, $\epsilon=0.15$, $\sigma=C=0$, and $L=301$, we plot the space-time state of the system in Fig. 10(a) in the same manner as in Fig. 2(c); a cluster of bursts appears without external forcing. In Fig. 10(b) we record the data of the time series of an arbitrary site ($i=1$); the on-off type of intermittency is clearly shown. Now the ''off'' state is the exact T2S2 state. In Fig. 10(c), the laminar phase distribution of (b) is presented, showing perfect critical $-\frac{3}{2}$ power-law decay. In Fig. 10(d), the laminar phase distribution averaged from the laminar phases of all the 301 sites, we get the same straight line with much fewer fluctuations.

It is not surprising to find bursts (or defects) from the T2S2 state in Fig. 10 since the odd number of cells does not fit the T2S2 state, and defects can be excited continually by an unmatched site. However, it is really surprising that similar behavior can be observed even if the basic laminar phase is spatiotemporal chaos. Figures 11(a)–11(d) are the same as Figs. 10(a)–10(d) except that the coupling strength is $\epsilon=0.125$ rather than 0.15. Therefore, the laminar phase is no longer the regular T2S2 periodic state. It is represented by the chaotic bands of Fig. 8(a). The on-off intermittency nature of the system dynamics can be clearly seen in Figs. 11(a) and 11(b) (note that the dynamic feature is the same for any site from $i=1$ to $i=301$ due to the symmetry of the CML). Perfect $-\frac{3}{2}$ power-law scaling is shown in Figs. 11(c) and 11(d), indicating that the characteristics of the criticality of on-off intermittency are the intrinsic properties of the motions of all the sites without external injection, when the system is in strong spatiotemporal chaos.

From Figs. 10 and 11, we can further understand the mechanism of the on-off intermittency in our model. With even L, there is a globally stable state for our CML model [the T2S2 state in Fig. 1(a) and the spatiotemporal chaotic state in Fig. 8(a)]. By injecting a small local force σ, we can change the system dynamics locally (since the original state is stable and most of the sites move in the vicinity of the original set). As the forcing strength exceeds a critical value, the system is driven to the boundary of a kind of instability. Over this critical value, bursts (defects) from this set are excited from the forced site and propagate in space. However, there is no other stable state for the system; all sites have a strong tendency to go back to the original positions through stable manifolds of the original set by way of defect pair annihilations [15,16]. With continual excitation by the local injection, the defect creation, propagation, and annihilation processes lead to the spatiotemporal intermittency. With odd L, there is always a site unmatched for the defect-pair annihilation, which serves as a source of defect excitation. Therefore, this on-off intermittency can persist without any local injection.

ACKNOWLEDGMENTS

This work was supported partially by the Chinese Natural Science Foundation, and Project of Nonlinear Science and the Open Laboratories Project of Academia Sinica. Sun Microsystems, Inc., donated a Workstation, and Wolfram Research, Inc., donated the MATHEMATICA software to the Nonlinear Dynamics Group at ITP.

[1] F. H. Willeboordse and K. Kaneko, Phys. Rev. Lett. **73**, 533 (1994).
[2] Qu Zhilin and Hu Gang, Phys. Rev. E **49**, 1099 (1994).
[3] K. Kaneko, Prog. Theor. Phys. **72**, 480 (1984); **74**, 1033 (1985); Physica D **23**, 436 (1986).
[4] J. P. Crutchfield and K. Kaneko, in *Directions in Chaos*, edited by Hao Bailin (World Scientific, Singapore, 1987), p. 272.
[5] K. Kaneko, Physica D **34**, 1 (1989).
[6] K. Kaneko, Phys. Lett. A **125**, 25 (1987); **149**, 105 (1990); Physica D **37**, 60 (1989).
[7] J. P. Crutchfield and K. Kaneko, Phys. Rev. Lett. **60**, 2715 (1988).
[8] P. Bak, Chao Tang, and K. Wiesenfeld, Phys. Rev. A **38**, 364 (1988).
[9] K. Chen and P. Bak, Phys. Rev. A **43**, 625 (1991).
[10] N. Platt, E. A. Spiegel, and C. Tresser, Phys. Rev. Lett. **70**, 279 (1993).
[11] J. F. Heagy, N. Platt, and S. M. Hammel, Phys. Rev. E **49**, 1140 (1994).
[12] P. W. Hammer, N. Platt, S. M. Hammel, J. F. Heagy, and B. D. Lee, Phys. Rev. Lett. **73**, 1095 (1994).
[13] N. Platt, S. M. Hammel, and J. F. Heagy, Phys. Rev. Lett. **72**, 3498 (1994).
[14] Fagen Xie, Gang Hu, and Zhilin Qu, Phys. Rev. E **52**, R1265 (1995).
[15] K. Kaneko, Europhys. Lett. **6**, 193 (1988).
[16] F. H. Willeboordse and K. Kaneko, Physica D **85**, 428 (1995).